TECHNICAL REPORT

Study of the road traffic noise prediction method applicable to low-noise road surfaces

Keisuke Tsukui[1], Yasuo Oshino[1], Gijsjan van Blokland[2] and Hideki Tachibana[3]

[1]*Japan Automobile Research Institute,*
2530, Karima, Tsukuba, 305–0822 Japan
[2]*M+P Noise and Vibration Consultancy,*
Wolfskamerweg 47, P.O.Box 2094, NL-5260 CB VUGHT, the Netherlands
[3]*Chiba Institute of Technology,*
2–17–1, Tsudanuma, Narashino, 275–0016 Japan

TECHNICAL REPORT

Study of the road traffic noise prediction method applicable to low-noise road surfaces

Keisuke Tsukui[1], Yasuo Oshino[1], Gijsjan van Blokland[2] and Hideki Tachibana[3]

[1]*Japan Automobile Research Institute,*
2530, Karima, Tsukuba, 305–0822 Japan
[2]*M+P Noise and Vibration Consultancy,*
Wolfskamerweg 47, P.O.Box 2094, NL-5260 CB VUGHT, the Netherlands
[3]*Chiba Institute of Technology,*
2–17–1, Tsudanuma, Narashino, 275–0016 Japan

Abstract: In this study, the new road traffic noise prediction method applicable to Japanese and Dutch various road surfaces was developed. Firstly, the A-weighted sound power levels of road vehicles were measured for actual roads in the Netherlands paved with various surfaces. With regard to the levels on dense asphalt concrete, the differences between Dutch and Japanese data were not significant, therefore it was found that the common sound power calculation model can be used in both Japan and the Netherlands. On the other hand, the levels for low-noise road surfaces in the Netherlands were 1 to 7 dB lower than those for dense asphalt concrete, therefore the different sound power calculation models were required to be constructed for such surfaces. Secondly, based on the above results, a sound power calculation model applicable to each road surface was developed. By integrating the model with the dynamic traffic flow calculation model, the new road traffic noise prediction method was constructed. Using the method, the road traffic noise in 32 urban areas including low-noise road surfaces in Japan and the Netherlands was calculated. As a result, the calculated levels correspond well with the measured levels (the differences between them were 1.3 dB on average).

1. INTRODUCTION

Recently, road traffic noise has been a serious problem worldwide, and countermeasures for road traffic noise are being actively examined, particularly in Japan and Europe. Road traffic noise prediction models are useful tools for the examination of countermeasures. Therefore, in Japan and Europe, respective prediction models are being developed [1–3]. To compare road traffic noise among various countries, or to internationalize the noise reduction measures, it would be effective to establish the road traffic noise prediction model applicable to both Japan and Europe. For this purpose, it is necessary to unify the estimation model for road vehicle noise between Japan and Europe. It is hypothesized that the tire/road noise greatly depends on the road surfaces paved in each country. Therefore, an examination of the effect of road surface is very important.

Furthermore, noise pollution is a serious problem especially in urban areas. As a solution, it is also desirable to establish the prediction model that is applicable to transient traffic flow in urban areas.

In Japan Automobile Research institute (JARI), the road traffic noise prediction method has been developed which combines the calculation model of transient running conditions in urban areas and the calculation model of the A-weighted sound power levels of road vehicles on various running conditions [4–8]. Since the power-unit noise and the tire/road noise of road vehicles are calculated separately in the model, it is technically possible to evaluate the effect of noise reduction by improving road surfaces. For this evaluation, it is necessary to develop the sound power calculation models applicable to various road surfaces.

In this study, JARI's road traffic noise prediction model was modified in order to estimate the road traffic noise in

urban areas paved with various types of road surfaces in different countries.

Firstly, the sound power levels of road vehicles were measured for actual roads in the Netherlands paved with various surfaces. Using these results, the sound power levels on the same type of road surface in Japan and the Netherlands were compared, followed by an examination of whether the sound power calculation model constructed in Japan was directly applied to the Netherlands or not.

Next, the noise reduction effects of Dutch low-noise road surfaces were studied, and subsequently the calculation model of the sound power levels applicable to each road surface was constructed.

Finally, the calculation model was introduced to JARI's road traffic noise prediction method. By using this method, road traffic noise in 32 urban areas including low-noise road surfaces in Japan and the Netherlands was estimated, and the accuracy of the prediction method was examined.

2. OUTLINE OF JARI's ROAD TRAFFIC NOISE PREDICTION METHOD

In the case of urban roads, traffic flow is interrupted by traffic signals, and the vehicle noise greatly changes due to vehicles' transient running conditions. Therefore, it is more difficult to predict the road traffic noise in such areas than that in steady flow conditions. In JARI, the traffic flow calculation model considering transient running conditions and the calculation model of the sound power levels in such running conditions was combined, and then the road traffic noise prediction method which is applicable to transient traffic flow as well as steady traffic flow was developed. In this chapter, the outline of the road traffic noise prediction method is described.

2.1. Calculation Model for Traffic Flow

Our prediction method adopts the dynamic traffic flow simulation model which combines the acceleration and deceleration patterns for individual vehicles with the car-following theory. In this model, when there is sufficient distance to the preceding vehicle, the following vehicle runs according to the running pattern for the individual vehicle. On the other hand, the following vehicle adjusts its speed according to the car-following theory to avoid a collision [7].

The acceleration and deceleration patterns for individual vehicles were measured using three types of vehicles (a passenger car, a light truck and a large-sized truck). From the measurement results, the approximate expressions for estimating the running patterns were constructed [4].

As a car-following model, the model based on Bando's model was adopted [7]. The accelerations of following vehicles are obtained as a function of the speeds of preceding vehicles, spacings between vehicles, and so on:

$$x''(t + \Delta t) = \alpha\{v_{\text{optimal}}(\Delta x) + v_{\text{lead}}(t) - 2v_{\text{follow}}(t)\} \quad (1)$$

$x''(t + \Delta t)$: acceleration (m/s^2) of a following vehicle at the time $t + \Delta t$

Δt: time interval (0.1 s)

v_{optimal}: optimal vehicle speed (m/s) under the condition Δx

Δx: spacing between a preceding vehicle and a following vehicle (m)

v_{lead}: speed of a preceding vehicle (m/s)

α: coefficient for a driver's response.

For the parameters v_{optimal} and α in Eq. (1), the measured values shown in reference [8] were used as follows:

$$v_{\text{optimal}}(\Delta x) = \frac{-b + \sqrt{b^2 - 4a(c - \Delta x)}}{2a} \quad (2)$$

$$a = 6.550 \times 10^{-3}$$

$$b = 1.218$$

$$c = 5.204$$

$$\alpha = 0.290. \quad (3)$$

Figure 1 shows an example of the simulated positions of vehicles in the vicinity of signalized intersections. The large and small rectangles in the figure indicate large-sized vehicles and passenger cars (or small-sized vehicles), respectively. During the time when the red light is on, from 0 s to 35 s, the number of vehicles waiting for the change in the signals increases, and during the proceeding time when the green light is on, vehicles start in order and traffic flow gradually changes from a transient condition to a steady flow condition. In this way, our simulation method
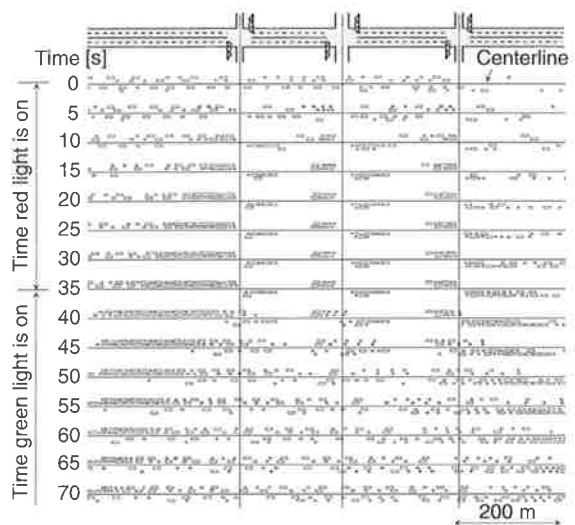

Fig. 1 Example of simulated traffic flow.

calculates the position and speed of each vehicle at every moment.

2.2. Basic Calculation Model of Each Vehicle's Sound Power Level

The noise generated by running vehicles can be mainly divided into two sources: power-unit noise and tire/road noise. The contribution of each noise source changes markedly with running conditions. In this study, by calculating these two kinds of noises separately then by combining them, the vehicle noise is estimated.

In order to develop the calculation model, a vehicle noise measurement test was conducted using three types of road vehicles on a test track. Its road surface conforms to ISO 10844 [9]. The power-unit noise and the tire/road noise were separately measured under various running conditions. The tire/road noise was measured by using the coasting test (in which the engine is switched off and the vehicle runs under its own inertia). The power-unit noise was obtained by subtracting the results of the coasting tests from those of normal running tests (in which the engine is operated normally). During the sound power measurement test, the vehicle speeds, the engine revolution speeds and engine loads were simultaneously measured.

From the measurement results, the approximate expressions for estimating the power-unit noise and the tire/road noise were constructed.

[Power-unit noise]

$$L_{WE} = C_{DE0} + C_{DE1} \log_{10} \frac{S}{S_0} + C_{DE2} T \qquad (4)$$

L_{WE}: A-weighted sound power level of the power-unit noise (dB)
 S: engine revolution speed (rpm)
 S_0: referenced engine revolution speed (1 rpm)
 T: engine load (%)
  C_{DE0}, C_{DE1}, C_{DE2}: regression coefficients.

[Tire/road noise]

$$L_{WT} = C_{DT0} + C_{DT1} \log_{10} \frac{V}{V_0} \qquad (5)$$

L_{WT}: A-weighted sound power level of the tire/road noise (dB)
 V: vehicle speed (km/h)
 V_0: referenced vehicle speed (1 km/h)
  C_{DT0}, C_{DT1}: regression coefficients.

Tire/road noise is calculated by substituting the vehicle speed (which is estimated by using the traffic flow simulation model described in the previous section), into Eq. (5). On the other hand, the calculation model of power-unit noise is given as a function of engine revolution speed and engine load, as described in Eq. (4). Therefore, the

Table 1 Regression coefficients in Eq. (4).

Vehicle type	Regression coefficients			Correlation coefficients
	C_{DE0}	C_{DE1}	C_{DE2}	
Passenger car	−14.22	30.52	0.0906	0.951
Small-sized vehicle	37.00	17.25	0.0490	0.890
Large-sized vehicle	23.39	24.25	0.0396	0.984

calculated result of the traffic flow simulation cannot be directly substituted into Eq. (4). Therefore in this study, using the procedure described in the Appendix, engine revolution speed and engine load are provisionally calculated from the speed and acceleration of each vehicle, then they are substituted into Eq. (4), thus, the power-unit noise is obtained.

The regression coefficients C_{DE0}, C_{DE1}, and C_{DE2} in Eq. (4) are shown in Table 1. The correlation coefficient for each vehicle type is greater than 0.89, therefore, it is found that Eq. (4) precisely estimates the power-unit noise of each vehicle. The discussion on the regression coefficients C_{DT0} and C_{DT1} in Eq. (5) are described in the next chapter.

2.3. Prediction of Road Traffic Noise

Figure 2 shows the flowchart of the road traffic noise prediction model in this study. Firstly, by using the dynamic traffic flow simulation model, the position, speed and acceleration of each vehicle are estimated. Secondly, engine revolution speed and engine load are calculated from each vehicle speed and acceleration using the vehicle motion equation described in the Appendix, then they are substituted into Eq. (4), thus, the power-unit noise L_{WE} is obtained. Also, each vehicle speed is substituted into Eq. (5) and the tire/road noise L_{WT} is calculated. Then, by introducing the vehicle noise directivity model [6], the sound propagation from each vehicle to the receiving point is calculated. In the calculation, each vehicle is assumed to be point source located at the center of the vehicle on the road surface [10]. Finally, by summing these results, the time series of A-weighted sound pressure levels at the receiving point are calculated, from which L_{Aeq} for a certain time-interval is calculated.

3. IMPROVEMENT OF VEHICLE'S SOUND POWER CALCULATION MODEL

In section 2.2, basic calculation model of sound power level developed by using three types of road vehicles was described. For actual roads, however, especially on various types of road surfaces in other countries, there is a possibility that the sound power levels are extremely different. In this chapter, therefore the sound power calculation model which is applicable to different countries
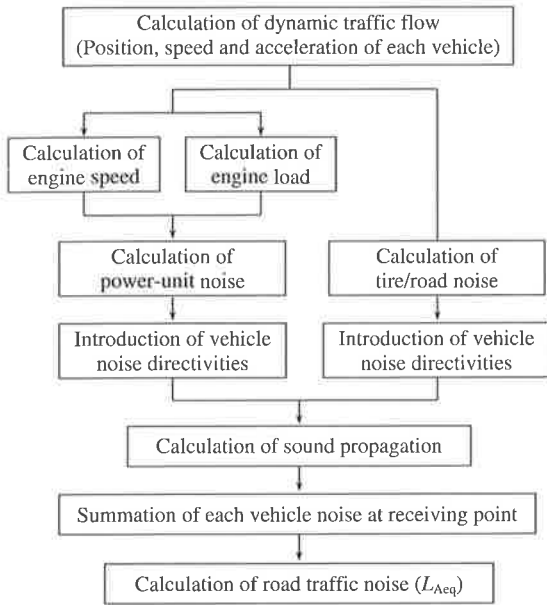
Fig. 2 Flowchart of the road traffic noise prediction model.

Table 2 Number of vehicles for sound power level measurements.

Road surface type	Passenger cars	Large-sized vehicles	Total
Dense asphalt	355	211	566
SMA 0/6	286	30	316
Microlayers	343	15	358
2-layer porous asphalt	333	36	369
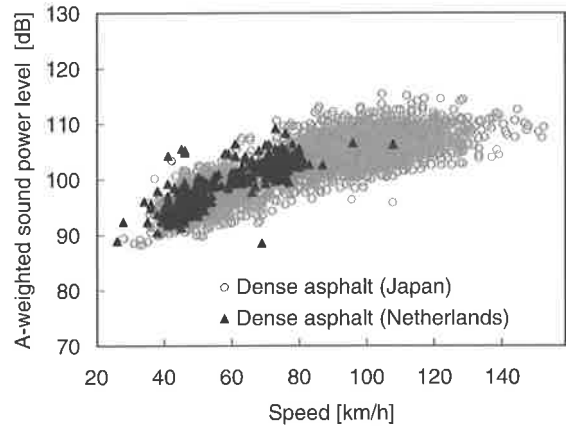
Fig. 3 Comparison of sound power levels on dense asphalt concrete (Passenger cars).

is developed. Firstly, pass-by noise of road vehicles was measured for actual roads in the Netherlands paved with various surfaces, then the result was compared with Japanese data. Secondly, by using these results, the improvement of the sound power calculation models described in section 2.2 (expansion of target road surfaces) was examined.

3.1. Measurement Method

In the vicinity of signalized intersections on urban roads, the sound power levels of road vehicles greatly change according to their engine revolution speeds and engine loads as well as vehicle speeds. Therefore, in such areas, it is difficult to examine precisely the sound power levels. In this study, firstly, the relationship between vehicle speeds and sound power levels was investigated in steady traffic areas. The procedure for extending the investigated results to the case of transient traffic areas is described in section 3.3.

The sound power level of a running vehicle was calculated from the FAST-maximum value of the A-weighted sound pressure level during pass-by [2]. The FAST-maximum value was measured by using a microphone located 7.5 m from the center of the running path and 1.2 m above the ground (according to ISO 11819-1 [11]). The vehicle speeds were measured using a radar-type speedometer. For the measurement areas, Dutch roads paved with dense asphalt concrete and three types of low-noise road surfaces (SMA 0/6, Microlayers and 2-layer porous asphalt), were chosen. The number of vehicles

measured for each road surface is shown in Table 2, where 1,600 data were obtained. However, the data of small-sized vehicles were not able to be obtained. This is due to in the Netherlands, small-sized vehicles in the Japanese vehicle category not being used as commonly as Japan.

3.2. Measurement Results

Among the road surface types investigated in the Netherlands, dense asphalt concrete has a common characteristic with Japan and its sound absorption characteristic is negligible, therefore vehicles' sound power levels can be compared on the same condition between Japan and the Netherlands. Firstly, the sound power levels on dense asphalt concrete in Japan and the Netherlands were compared, followed by an examination whether the sound power calculation model constructed in Japan was directly applied to the Netherlands or not.

Figure 3 shows the relationship between vehicle speed and sound power level for passenger cars. In the figure, black triangles indicate the results of sound power level for dense asphalt concrete measured in the Netherlands and gray circles indicate those measured in Japan (published by the Acoustical Society of Japan [2]). The sound power levels for dense asphalt concrete in the Netherlands and Japan are almost the same.

Table 3 Regression coefficients C_{V0} and C_{V1} in Eq. (6).

	Dense asphalt (Japan)	Dense asphalt (Netherlands)
C_{V0}	44.6	43.8
C_{V1}	30.4	31.5

It was reported that sound power levels under steady running conditions mainly depend on the vehicle speeds and that they can be precisely calculated by the function of vehicle speed [2]. Therefore in order to model the vehicles' sound power levels on the road surfaces in Japan and the Netherlands, the sound power levels were approximated by the function of vehicle speed as follows:

$$L_W = C_{V0} + C_{V1} \log_{10} \frac{V}{V_0} \tag{6}$$

L_W: A-weighted sound power level of running vehicle noise (dB)

V: vehicle speed (km/h)

V_0: referenced vehicle speed (1 km/h)
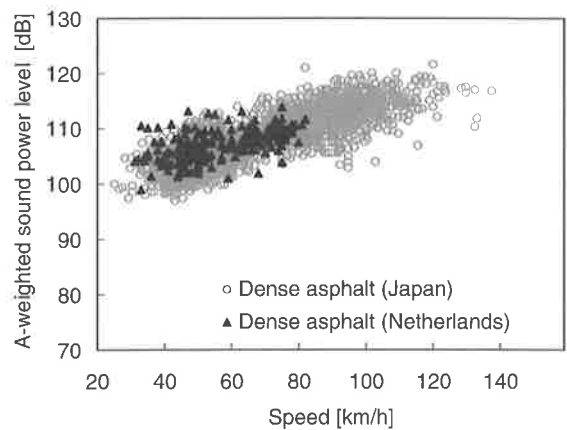
C_{V0}, C_{V1}: regression coefficients.

By using the data shown in Fig. 3, regression analysis between vehicle speed and sound power level was conducted. The results of the regression coefficients C_{V0} and C_{V1} are shown in Table 3. The coefficients have a similar tendency between Japan and the Netherlands (its quantitative analysis is described later). Furthermore, the coefficients C_{V1} which indicates the dependency on vehicle speed, are approximately 30 for both of countries.

Figure 4 shows the relationship between vehicle speed and sound power level for large-sized vehicles. The Dutch data seems to be slightly higher than the Japanese data, nevertheless the differences are not significant.

The regression coefficients in Eq. (6) were derived by using the Japanese data shown in Fig. 4. As a result, the coefficient C_{V1} which indicates the dependency on vehicle speed is approximately 30 (29.1). This result is similar to the case of passenger cars. Whereas in case of Dutch data, a clear dependency of sound power level on vehicle speed wasn't observed, since Dutch data distribute within a narrow speed range (in Europe it is impossible for most large-sized vehicles to run faster than 90 km/h due to speed limiters which have been introduced much earlier than Japan).

Therefore, for simplification in this study, the regression coefficient C_{V1} is assumed to be 30 for both of passenger cars and large-sized vehicles and for both of Japanese and Dutch road surfaces.

Table 4 shows the regression coefficients C_{V0} in Eq. (6) when C_{V1} is fixed at 30. For both passenger cars and large-sized vehicles, the sound power levels in the Netherlands are slightly higher than those in Japan.

Fig. 4 Comparison of sound power levels on dense asphalt concrete (Large-sized vehicles).

Table 4 Regression coefficients C_{V0} in Eq. (6). (On dense asphalt concrete in Japan and the Netherlands)

Vehicle type	Dense asphalt (Japan)	Dense asphalt (Netherlands)
Passenger cars	46.4	47.7 [1.3]
Large-sized vehicles	53.2	54.3 [1.1]

*The numbers in brackets indicate the differences from the data on dense asphalt concrete in Japan

However, the differences between Dutch data and Japanese data are approximately 1 dB. From the results, for the simplification in the following analysis, the sound power level on Japanese dense asphalt concrete is used as the standard level.

3.3. Sound Power Levels Measured on Dutch Low-Noise Road Surfaces

Sound power levels measured on Dutch low-noise road surfaces were compared to the data measured on dense asphalt concrete in Japan, and then the noise reduction effects of Dutch low-noise road surfaces were studied.

Figure 5 shows the relationship between vehicle speed and sound power level for passenger cars. Sound power levels on three types of low-noise road surfaces (SMA 0/6, Microlayers and 2-layer porous asphalt) distribute a relatively lower range compared with those on dense asphalt concrete.

These sound power levels were approximated by using Eq. (6) and the regression coefficients C_{V0} and C_{V1} shown in Table 5. In the same way as for dense asphalt concrete, the coefficient C_{V1} which indicates the dependency on vehicle speeds is approximately 30 for the low noise road surfaces.
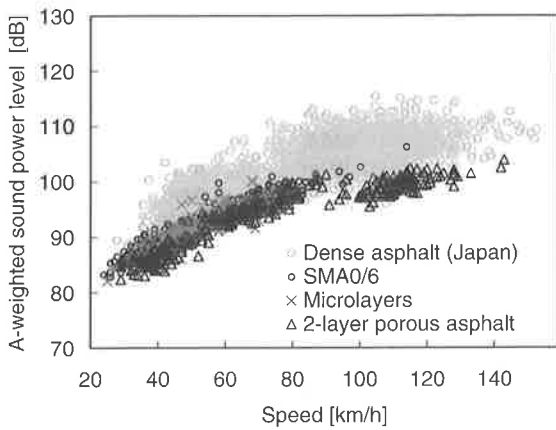
Fig. 5 Comparison of sound power levels on different road surfaces (Passenger cars).
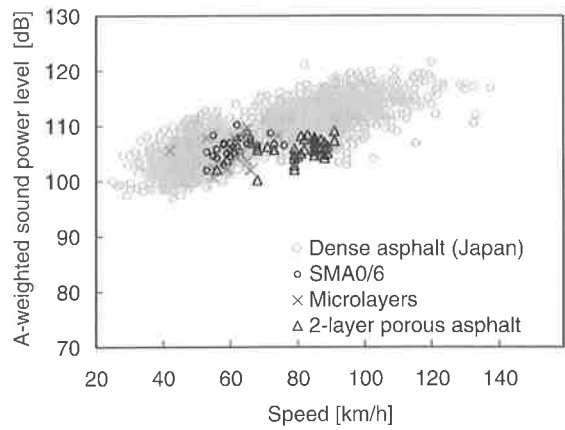
Table 5 Regression coefficients C_{V0} and C_{V1} in Eq. (6) (Passenger cars).

	Dense asphalt	SMA 0/6	Microlayers	2-layer porous asphalt
C_{V0}	44.6	39.5	35.0	41.1
C_{V1}	30.4	30.9	33.0	28.8

Fig. 6 Comparison of sound power levels on different road surfaces (Large-sized vehicles).

Table 6 Regression coefficients C_{V0} in Eq. (6).

Vehicle type	Dense asphalt	SMA 0/6	Microlayers	2-layer porous asphalt
Passenger cars	46.4	42.3 [−4.1]	41.0 [−5.4]	39.8 [−6.6]
Large-sized vehicles	53.2	52.1 [−1.1]	51.5 [−1.7]	47.9 [−5.3]

*The numbers in brackets indicate the differences from the data on dense asphalt concrete in Japan

Figure 6 shows the relationship between vehicle speed and sound power level for large-sized vehicles. Noise reduction effects of SMA0/6 and Microlayers are not clearly observed in this figure, whereas it is seen that the sound power levels on 2-layer porous asphalt are generally lower than those for the dense asphalt concrete. Incidentally, Dutch data doesn't show a clear dependency on vehicle speeds, due to distribution being within a narrow speed range.

Therefore, in order to quantify the noise reduction effects of the low-noise road surfaces, in the same way as section 3.2, the regression coefficient C_{V0} in Eq. (6) for each road surface was compared in the case when the regression coefficient C_{V1} for all of the surface types is fixed at 30 for both of passenger cars and large-sized vehicles. The result is shown in Table 6. The levels for low-noise road surfaces in the Netherlands are lower than those for dense asphalt concrete in Japan. The differences are 4.1 to 6.6 dB for passenger cars and 1.1 to 5.3 dB for large-sized vehicles. In the case when the levels for the low-noise road surfaces are compared with those for Dutch dense asphalt concrete, the differences are 5.4 to 7.9 dB for passenger cars and 2.2 to 6.4 dB for large-sized vehicles. From these results, it was found that the different sound power calculation models were required to be constructed for the three types of low-noise road surfaces.

3.4. Calculation Model of Sound Power Levels on Various Road Surfaces

As described above, the vehicles' sound power calculation model in this study estimates power-unit noise and the tire/road noise separately.

The power-unit noise change can be neglected even if the road surface changes. On the other hand, the tire/road noise changes markedly with the difference of road surface type. Therefore, in order to estimate vehicle noise on various road surfaces, the sound power levels of tire/road noise (which correspond to the regression coefficients C_{DT0} and C_{DT1} in Eq. (5)) were obtained as follows.

1) For each vehicle speed, the sound power level of the power-unit noise in steady running condition is calculated by using the method described in section 2.2.

2) For each vehicle speed, the sound power levels of road vehicles are calculated using Eq. (6) for each road surface (C_{V1} is fixed at 30 and the results of Table 6 are substituted for C_{V0}).

3) The sound power level of the tire/road noise for each road surface is calculated by subtracting the sound power level of the power-unit noise calculated in 1) from that of running vehicles calculated in 2).

Table 7 Regression coefficients C_{DT0} in Eq. (5).

Vehicle type	Dense asphalt	SMA 0/6	Microlayers	2-layer porous asphalt
Passenger cars	44.8	40.4	39.4	38.2
Small-sized vehicles	44.3	39.9	38.9	37.7
Large-sized vehicles	52.0	50.9	50.3	46.7

4) By using the results in 3), the regression coefficients C_{DT0} and C_{DT1} in Eq. (5) are obtained.

For small-sized vehicles, the sound power levels of running vehicles were not obtained as mentioned in section 3.1. Therefore C_{DT0} and C_{DT1} in Eq. (5) for small-sized vehicles are estimated by using the assumptions as follows:

a) The sound power levels for small-sized vehicles on dense asphalt concrete are calculated by using Japanese data [2] in the same way as passenger cars and large-sized vehicles. Under this assumption, the sound power levels for small-sized vehicles are 1.2 dB higher than those for passenger cars.

b) The sound power levels for small-sized vehicles on the other road surfaces are also assumed to be 1.2 dB higher than those for passenger cars.

c) By using the assumption a) and b), and the procedure 1) to 4) in this section, C_{DT0} and C_{DT1} for small-sized vehicles are estimated.

Using the data for each vehicle type, the regression coefficients C_{DT0} and C_{DT1} were calculated. As a result, the regression coefficients C_{DT1} were approximately 30 (from 30.0 to 33.3). Therefore, for simplification in this study, the regression coefficient C_{DT1} is assumed to be 30 under all conditions. Table 7 shows the regression coefficient C_{DT0} in Eq. (5) when C_{DT1} is fixed at 30. For each vehicle type, the regression coefficients on the low-noise surfaces are lower than those on dense asphalt concrete.

In this study, the difference in tire/road noise due to road surface type is taken into account by using the regression coefficients C_{DT0} in Table 7.

4. VALIDATION OF THE ROAD TRAFFIC NOISE PREDICTION MODEL

To examine the validity of our prediction method, the road traffic noise for urban roads paved with various surfaces in the Netherlands and Japan was calculated, and the results were compared with the measured data.

4.1. Road Traffic Noise Prediction Areas

Twenty urban areas around Eindhoven, 's-Hertogenbosch, the Hague, Tilburg and Beuningen in the Netherlands, and twelve urban areas around Tokyo in Japan were selected, and traffic volumes of each vehicle type, road surface types and road traffic noise $L_{Aeq,15min}$ were investigated. The road traffic noise was measured

Table 8 Road surface types of measured locations.

Location	Distance from traffic lights	Road surface types
No. 1	40 m	SMA 0/6
No. 2	250 m	dense asphalt concrete
No. 3	180 m	dense asphalt concrete
No. 4	200 m	dense asphalt concrete
No. 5	200 m	dense asphalt concrete
No. 6	200 m	Microlayers
No. 7	250 m	dense asphalt concrete
No. 8	180 m	SMA 0/11
No. 9	250 m	SMA 0/11
No. 10	180 m	SMA 0/11
No. 11	100 m	dense asphalt concrete
No. 12	120 m	dense asphalt concrete
No. 13	≥500 m	dense asphalt concrete
No. 14	200 m	dense asphalt concrete
No. 15	150 m	dense asphalt concrete
No. 16	30 m	dense asphalt concrete
No. 17	200 m	dense asphalt concrete
No. 18	30 m	dense asphalt concrete
No. 19	250 m	2-layer porous asphalt
No. 20	150 m	Microlayers
No. A	25 m	
No. B	25 m	
No. C	100 m	
No. D	60 m	
No. E	50 m	
No. F	≥500 m	
No. G	30 m	dense asphalt concrete
No. H	≥500 m	
No. I	≥500 m	
No. J	≥500 m	
No. K	≥500 m	
No. L	180 m	

1.2 m above the ground at the roadside. The road surface types at the measurement areas and the distance from the nearest traffic lights to the measurement points are shown in Table 8. Locations No. 1 to No. 20 are the areas in the Netherlands, and locations No. A to No. L are those in Japan. The number of road surface types measured in the Netherlands was five: dense asphalt concrete, SMA 0/6 (maximum chipping size: 6 mm), SMA 0/11 (maximum chipping size: 11 mm), Microlayers and 2-layer porous asphalt. All the road surfaces in Japan were dense asphalt concrete.

The investigated results of road traffic noise $L_{Aeq,15min}$, total traffic volume and the traffic volume of large-sized vehicles are shown in Fig. 7. The rate of occurrence of the large-sized vehicles and the total traffic volume in the Netherlands are commonly lower than those in Japan. Therefore, road traffic noise in the Netherlands is generally lower than that in Japan. One of the reasons for this might be the sufficient provision of expressways or by-pass roads around city areas and physical distribution systems, such as truck terminals, in the Netherlands.
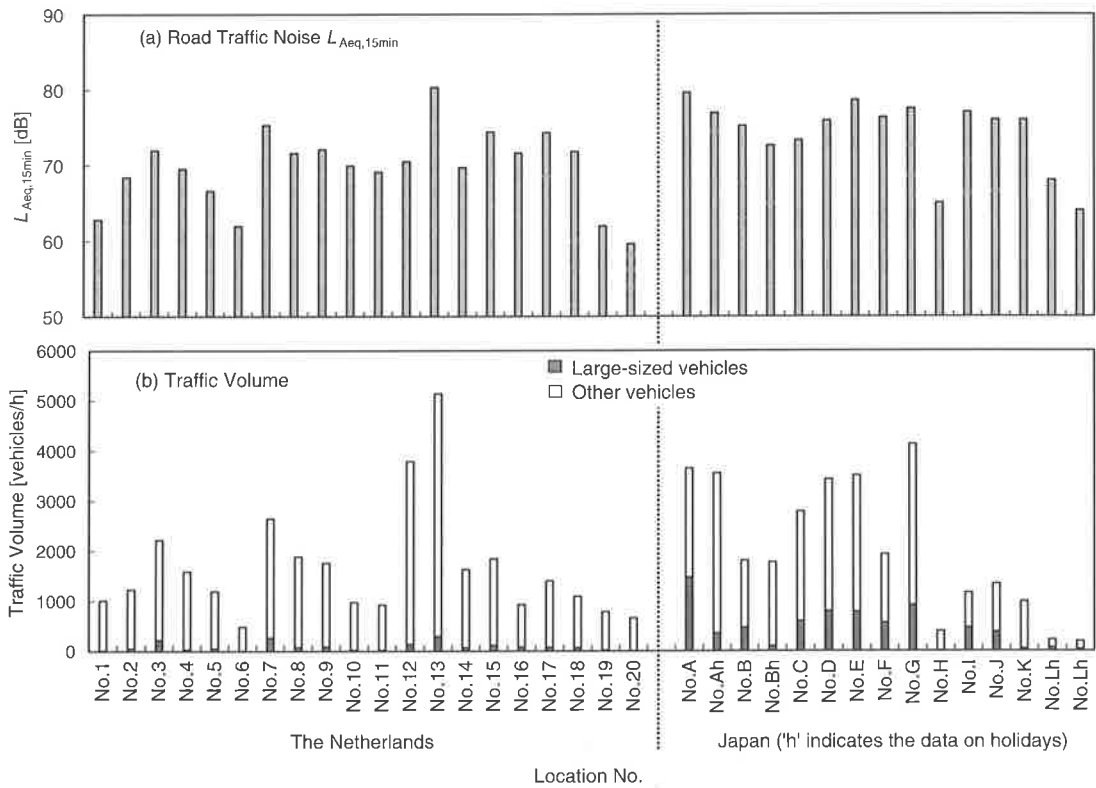
Fig. 7 $L_{Aeq,15min}$ and traffic volume measured in the Netherlands and Japan.

4.2. Calculated Results

The traffic conditions, road width, the numbers of lanes, positions of traffic lights and road surface types of the investigated areas were introduced into the road traffic noise prediction method and $L_{Aeq,15min}$ was calculated. In the investigated areas, there are three roads paved with SMA 0/11. To predict $L_{Aeq,15min}$ for SMA 0/11, the sound power calculation model on dense asphalt concrete was used, because it was reported that the sound power levels of road vehicles on SMA 0/11 are similar to those on dense asphalt concrete [12]. Figure 8 shows a comparison between the calculated and measured $L_{Aeq,15min}$. Grey circles in the figure indicate the results for Japan, and the other marks indicate those for the Netherlands. In the figure, the calculated levels for Dutch dense asphalt concrete (white circles) tend to be distributed in slightly lower range than the measured levels. It is considered that this tendency is mainly caused by the assumption in which the sound power calculation models for Japanese dense asphalt concrete is directly applied to the case for Dutch dense asphalt concrete. However, for both roads in the Netherlands and Japan, the calculated values generally correspond well with the measured ones. The average of the differences (the absolute values) between the calculated
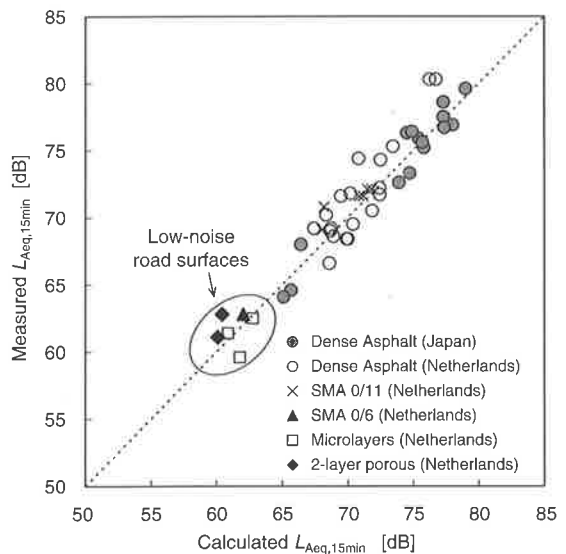

Fig. 8 Relationship between measured and calculated $L_{Aeq,15min}$.

and the measured levels is 1.3 dB (standard deviation is 0.9 dB). In particular, it is found that this prediction method is also applicable to the urban roads in the Netherlands

paved with low-noise road surfaces such as SMA 0/6, Microlayers and 2-layer porous asphalt. From the results, it is found that the prediction method developed in this study has the possibility of being applied to road traffic noise prediction for Dutch and Japanese urban roads paved with various surfaces.

5.   CONCLUSION

In this study, the road traffic noise prediction method applicable to urban roads paved with various surfaces was examined.

First, the sound power levels of road vehicles were measured for actual roads in the Netherlands paved with various surfaces. With regard to the sound power levels on dense asphalt concrete, the differences between Dutch and Japanese data were not significant, therefore it was found that the common sound power calculation model can be used in both of Japan and the Netherlands. Whereas the levels for low-noise road surfaces in the Netherlands were 1 to 7 dB lower than those for dense asphalt concrete, it was found that the different sound power calculation models were required to be constructed.

On the basis of the results, the calculation model of the sound power levels applicable to each road surface was constructed. Then, the model was integrated with the traffic flow calculation model considering the transient running condition of road vehicles, and the new road traffic noise prediction method has been developed.

Using the prediction method, the road traffic noise in 32 urban areas including low-noise road surfaces in Japan and the Netherlands was calculated. As a result, the calculated levels correspond well with the measured levels (the differences between them were 1.3 dB on average). Therefore, it can be expected that there is a possibility that the prediction model developed in this study is applicable to Dutch and Japanese urban roads paved with various types of surfaces.

REFERENCES

[1] H. Tachibana and K. Yamamoto, "Road traffic noise prediction model "ASJ RTN-Model 2003" proposed by the Acoustical Society of Japan — Part 1: The framework and the calculation scheme," *Proc. ICA 2004*, CD-ROM (2004).

[2] Y. Oshino, S. Kono, T. Iwase, H. Ohnishi, T. Sone and H. Tachibana, "Road traffic noise prediction model "ASJ Model 1998" proposed by the Acoustical Society of Japan — Part 2: Calculation model of sound power levels of road vehicles," *Proc. Inter-noise 2000*, pp. 3081–3086 (2000).

[3] H. G. Jonasson, G. Watts, U. Sandberg, J. Ejsmont, G. van Blokland, M. Luminari and J. D. van der Toorn, "The Harmonoise source model for road vehicles," *Proc. Inter-noise 2004*, paper No. 166 (2004).

[4] Y. Oshino and H. Tachibana, "Prediction of road traffic noise taking account of transient running conditions of vehicles," *Proc. Inter-noise 93*, pp. 629–632 (1993).

[5] H. Tachibana and Y. Oshino, "Road traffic noise prediction taking account of transient vehicle running conditions," *Proc. Inter-noise 96*, pp. 3117–3120 (1996).

[6] K. Tsukui, Y. Oshino and H. Tachibana, "Road traffic noise simulation model taking account of vehicle noise directivities," *Proc. Inter-noise 98*, paper No. 409 (1998).

[7] T. Suzuki, K. Tsukui, Y. Oshino and H. Tachibana, "Road traffic noise prediction model around signalized intersections," *Proc. Inter-noise 2003*, pp. 1870–1873 (2003).

[8] T. Suzuki, Y. Oshino and H. Tachibana, "Road traffic noise prediction model around signalized intersections taking account of right- and left-turn traffic," *J. Acoust. Soc. Jpn. (J)*, **60**, 526–535 (2004) (in Japanese).

[9] International Organization for Standardization, "ISO 10844:1994 Acoustics — Specification of test tracks for the purpose of measuring noise emitted by road vehicles —," *ISO* (1994).

[10] H. Tachibana and Y. Oshino, "Sound intensity radiation patterns of actually running automobiles," *Proc. Inter-noise 92*, pp. 849–852 (1992).

[11] International Organization for Standardization, "ISO 11819-1:1997 Acoustics — Measurement of the influence of road surfaces on traffic noise — Part 1: Statistical Pass-By method," *ISO* (1997).

[12] H. Jonasson, U. Sandberg, G. van Blokland, J. Ejsmont, G. Watts and M. Luminari, "Work Package 1.1 Source modeling of road vehicles, Deliverable 9 of the Harmonoise project, HAR11TR-041210-SP10 (2004-12-17)." (online), available from <http://www.imagine-project.org/bestanden/D09_WP1.1_HAR11TR-041210-SP10.pdf> (accessed 2007).

[13] The Society of Automotive Engineers of Japan, *Automotive Engineering Handbook*, 2nd ed. (The Society of Automotive Engineers of Japan, Tokyo, 1982) (in Japanese).

[14] The Society of Automotive Engineers of Japan, *Automotive Engineering Handbook Vol. 1 The Basic and Theoretical Edition* (The Society of Automotive Engineers of Japan, Tokyo, 1990) (in Japanese).

APPENDIX: ESTIMATION PROCEDURE FOR ENGINE REVOLUTION SPEED AND ENGINE LOAD

In this study, the engine revolution speed and engine load of each vehicle were calculated from the vehicle speed and acceleration using the vehicle motion equation [13,14]. The estimation procedure is as follows.

(1) Estimation procedure for engine revolution speed

The engine revolution speed is calculated from the vehicle speed and the vehicle specification as follows:

$$S = \frac{\rho_i \, \rho_f}{2\pi r} V \, 60 \qquad (A \cdot 1)$$

S: engine revolution speed (rpm)

ρ_i: gear ratios on gear position i $(i = 1, 2, \ldots)$

ρ_f: final gear ratio

r: radius of tire (m)

V: vehicle speed (km/h).

(2) Estimation procedure for engine load

From the vehicle motion equation, the relationship between the driving force and the vehicle acceleration is

$$\frac{W + \Delta W_i}{g} \frac{dv}{dt} = F - R \tag{A·2}$$

W: vehicle weight (kgf)

ΔW_i: equivalent vehicle weight of rotating parts at gear position i (kgf)

g: acceleration due to gravity ($9.8\,\text{m/s}^2$)

v: vehicle speed (m/s)

F: driving force (kgf)

R: running resistance (kgf).

The driving force F in Eq. (A·2) is calculated from the engine torque T_E as follows:

$$F = \frac{1}{r} \rho_i \rho_f \eta T_E \tag{A·3}$$

η: transmission efficiency

T_E: engine torque (kgfm).

The running resistance R in Eq. (A·2) is calculated using

$$R = \mu_r W + \mu_A A V^2 + W \sin\theta \tag{A·4}$$

μ_r: coefficient of rolling resistance

μ_A: coefficient of air resistance

A: frontal projected area (m)

θ: inclination angle (rad).

From Eqs. (A·2), (A·3) and (A·4), the engine torque T_E is calculated from the vehicle speed and acceleration as follows:

$$T_E = \frac{r}{\rho_i \rho_f \eta} \left\{ \frac{W + \Delta W_i}{g} \frac{dv}{dt} + \mu_r W + \mu_A A V^2 + W \sin\theta \right\} \tag{A·5}$$

The engine load T is calculated from the engine torque T_E using

$$T = \frac{T_E}{T_{max}} \times 100 \tag{A·6}$$

T: engine load (%)

T_{max}: maximum engine torque (kgfm).

The parameters in Eqs. (A·5) and (A·6) for the test vehicles are shown in Table A.1.

(3) Estimation procedure for engine revolution speed and engine load of vehicles on actual roads

There are many vehicles running on actual roads and their specifications are diverse. In this study their specifi-

cations are assumed to be represented by those of the three vehicles used in the noise test (see Table A.1). The values ρ_i and ΔW_i in the Tables vary step by step with changes in the gear positions. Therefore, the variance of vehicle speed at which the gear position was changed was set for each vehicle type. Table A.2 shows the averaged speed range for each gear position obtained from the investigated results of the running patterns on actual roads. Using the results, the gear position for arbitrary vehicle speed is calculated.

Table A.1 Parameters in Eqs. (A·5) and (A·6).

		Passenger car	Small-sized vehicle	Large-sized vehicle
W [kgf]		1,629	3,205	18,185
ΔW_i [kgf]	1st	2,769	4,968	—
	2nd	880	1,474	28,187
	3rd	326	641	8,365
	4th	163	288	3,637
	5th	133	239	1,637
	6th	116	—	1,296
η		0.92	0.92	0.92
ρ_i	1st	3,874	5.146	—
	2nd	2.175	2.780	4.389
	3rd	1,484	1.509	2.495
	4th	1.223	1.000	1.592
	5th	1.000	0.830	1.000
	6th	0.869	—	0.792
ρ_f		4.100	4.875	6.833
r		0.304	0.360	0.508
μ_r		0.015	0.013	0.007
μ_A		0.0020	0.0027	0.0032
A [m^2]		1.8	2.7	7.5
T_{max} [kgfm]		22.0	19.2	143.0

Table A.2 Speed range for each gear position.

Gear position	Speed range [km/h]		
	Passenger car	Small-sized vehicle	Large-sized vehicle
1st	0–27	0–18	—
2nd	27–42	18–34	0–18
3rd	42–50	34–54	18–33
4th	50–60	54–60	33–46
5th	60–75	60–	46–60
6th	75–	—	60–

Keisuke Tsukui was graduated from Faculty of Science and Technology, Sophia University in 1988, and received Engineering Doctor from Kanazawa University in 2008. He is a senior researcher with Japan Automobile Research Institute. His major is automotive engineering and acoustical engineering.

Yasuo Oshino was graduated from Science University of Tokyo in 1972, and received Engineering Doctor from University of Tokyo in 1993. He is a senior chief researcher with Japan Automobile Research Institute. He received the Prizes of Society of Automotive Engineers of Japan for Research Theses in 1987 and 1990.

Gijsjan van Blokland graduated in 1979 from Faculty of Physics and Mathematics of the Amsterdam University and received a PhD in Physics from the Utrecht University in 1986. Since then he works as a senior consultant at M+P Consulting engineers in Holland with the focus on sources of road and railway noise. Since 1997 he is the general manager of M+P and partner of the holding Müller-BBM AG in Germany.

Hideki Tachibana was graduated from Faculty of Engineering, University of Tokyo in 1967, and received Engineering Doctor from University of Tokyo in 1973. Professor of General Research Institute, Chiba Institute of Technology. Professor emeritus of University of Tokyo. President, ASJ, 1995–1997; President, INCE/Japan 2002–2004; President, International INCE, 2004–2008; Fellow, ASA, 1996–; Prize of the Architectural Institute of Japan, 1990; Prizes of ASJ, 1991, 2009, Lord Rayleigh Medal (IOA), 2002.